Solar Energy Materials and Solar Cells 200 (2019) 109953

Contents lists available at ScienceDirect

Solar Energy Materials and Solar Cells

journal homepage: www.elsevier.com/locate/solmat

Rear-emitter silicon heterojunction solar cells with atomic layer deposited ZnO:Al serving as an alternative transparent conducting oxide to In_2O_3:Sn

Janne-Petteri Niemelä[a,*,1], Bart Macco[a,**], Loris Barraud[b], Antoine Descoeudres[b], Nicolas Badel[b], Matthieu Despeisse[b], Gabriel Christmann[b], Sylvain Nicolay[b], Christophe Ballif[b,c], Wilhelmus M.M. Kessels[a,d], Mariadriana Creatore[a,d]

[a] Department of Applied Physics, Eindhoven University of Technology, PO Box 513, 5600 MB Eindhoven, the Netherlands
[b] Centre Suisse d'Électronique et de Microtechnique (CSEM), PV-center, Jaquet-Droz 1, CH-2000, Neuchâtel, Switzerland
[c] Institute of Microengineering (IMT) Photovoltaics and Thin-Film Electronics Laboratory (PV-Lab), Ecole Polytechnique Fédérale de Lausanne (EPFL), Rue de la Maladière 71b, 2002 Neuchâtel, Switzerland
[d] Solliance, High Tech Campus 21, 5656 AE, Eindhoven, the Netherlands

ARTICLE INFO

Keywords:
Transparent conducting oxide
Silicon heterojunction solar cell
Rear emitter solar cell
Zinc oxide
Atomic layer deposition

ABSTRACT

Here high-efficiency (above 21%) large-area silicon heterojunction solar cells with atomic layer deposited ZnO:Al as front- or back-side transparent conducting oxide are demonstrated. Photoconductance decay measurements indicate that the excellent chemical passivation provided by the *a*-Si:H(i,p) and *a*-Si:H(i,n) stacks is preserved upon deposition of ZnO:Al, and that field-effect passivation losses for the *a*-Si:H(i,p)/ZnO:Al contact can be mitigated by lowering the Al doping level. Use of low Al-doping is enabled by the rear-emitter configuration which, in addition to facilitating the *a*-Si:H(i,p)/ZnO:Al contact engineering, enables a higher photocurrent due to the decrease in free-carrier absorption in ZnO:Al. The results encourage the use of In-free transparent conducting oxides in silicon heterojunction solar cells, as the replacement of In_2O_3:Sn without efficiency loss is demonstrated.

Silicon heterojunction (SHJ) solar cells are an industrially viable technology with the record efficiency of 26.6% (demonstrated by using interdigitated back contacts) [1,2]. Operation of the SHJ cells relies on junctions between the crystalline silicon (*c*-Si) absorber and hydrogenated amorphous silicon (*a*-Si:H) layers [3]. While intrinsic *a*-Si:H provides chemical passivation of Si dangling bonds present at the surface of *c*-Si, n-type and p-type doped *a*-Si:H layers enable downward and upward band bending near the junctions (field-effect passivation), and serve as the electron-selective and the hole-selective layers, respectively. Transparent conducting oxide (TCO) layers are employed to contact the doped *a*-Si:H layers to metal contacts, that complete the cell design. Excellent surface passivation provided by the *a*-Si:H layer stacks is the key to high open circuit voltage (V_{oc}) values [4], which clearly should not be compromised during the TCO (and metal) deposition steps.

The current TCO material of choice is sputter-deposited In_2O_3:Sn (ITO) largely owing to its relatively high carrier mobility and the technological maturity in its usage [3,5–7]. However, the damage to the chemical passivation during the sputtering process [8] and scarcity of indium make the search of alternatives highly required. Although ZnO-based materials (doped intrinsically through presence of oxygen vacancies or extrinsically e.g. with aluminum, boron or hydrogen) have lower mobility than ITO, their earth abundance makes them viable material alternatives [9]. Indeed, encouraging results have already been obtained for sputter-deposited ZnO:Al (AZO; with nanocrystalline n-type Si:H electron-selective layer) [10]. Chemical-vapor based techniques such as atomic layer deposition (ALD) are interesting deposition-technique alternatives owing to their low-damage character. In this context, the influence of ALD deposition of ZnO:Al (AZO) on the quality of *a*-Si:H-based passivation has already been studied, and it was found out that the chemical passivation can indeed be preserved upon the deposition [11]. However, deterioration of the field-effect passivation lead to fill-factor losses [11], a drawback that could relate to the front-emitter cell design used in that work and the low mobility of AZO. In

* Corresponding author.
** Corresponding author.
E-mail addresses: j.niemela@tue.nl (J.-P. Niemelä), b.macco@tue.nl (B. Macco).
[1] Present address: Empa (Swiss Federal Laboratories for Materials Science and Technology), Feuerwerkerstrasse 39, 3602 Thun, Switzerland. Email: janne-petteri.niemelae@empa.ch

https://doi.org/10.1016/j.solmat.2019.109953
Received 10 January 2019; Received in revised form 27 April 2019; Accepted 14 May 2019
Available online 23 May 2019

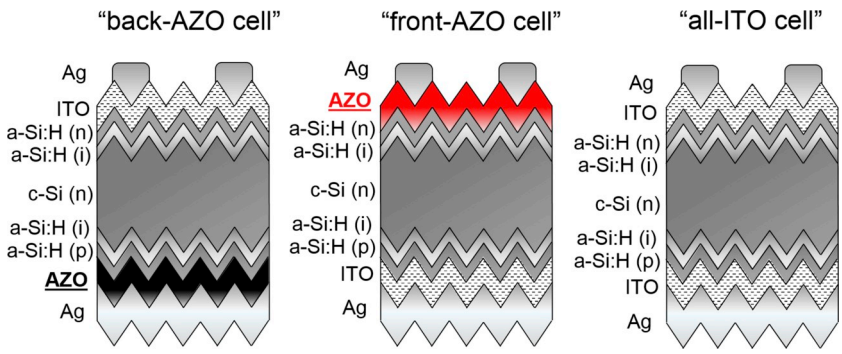

Fig. 1. The used rear-emitter SHJ-cell designs differing in terms of their TCOs: "back-AZO cell", "front-AZO cell" and "all-ITO cell". In all the cells *c*-Si(*n*) is the absorber layer, *a*-Si:H(*i*) provides the surface passivation, and *a*-Si:H(*n*) and *a*-Si:H(*p*) are the electron-selective and hole-selective layers, respectively. Ag is used as the metal contact material.

the front-emitter (n-type-absorber) cell design the *a*-Si:H(p) emitter is at the front of the cell, which requires a low-resistivity TCO for efficient lateral charge transport to the metal grid. When AZO is used as the TCO, low resistivity has to be reached by increasing the carrier density via high Al doping, owing to the low mobility of the material. High doping of a TCO in turn increases workfunction mismatch at the TCO/*a*-Si:H(p) interface and hence deteriorates the field-effect passivation [12]. High doping moreover increases free-carrier absorption in the vis-NIR range, which inevitably leads to a resistivity-transparency tradeoff [13]. These problems for the front contact could be mitigated by placing the *a*-Si:H(p) emitter at the rear of the cell [14,15].

We report here on the application of ALD AZO thin films in a SHJ cell design tailored to minimize the transparency-resistivity tradeoff and the field-effect passivation losses. By using monofacial rear-emitter solar cells, the conductivity requirement for the front-side AZO layer is relaxed as some of the current spreading is carried out by the n-type wafer, while at the back the current spreading is carried out by full-area metallization. This allows the use of low Al doping at both the front-side and the back-side of the cell. Consequently, more transparent AZO can be used and the field-effect passivation losses at the TCO/*a*-Si:H(p) interface can be mitigated. Using this configuration we demonstrate that ITO can be replaced by AZO without performance losses in large-area (100 cm^2) SHJ solar cells.

The solar cells were fabricated as follows. First 150-μm-thick n-type *c*-Si (Czochralski) wafers were etched in KOH to obtain a random pyramid surface texture; this step was followed by cleaning and native oxide removal. Then plasma-enhanced chemical vapor deposition (PECVD; Indeotec Octopus II reactor) was used to deposit *a*-Si:H(i) layers of about 10 nm thickness on both sides of the wafer, and subsequently, 10-nm *a*-Si:H(n) and 15-nm *a*-Si:H(p) layers were deposited at the front and at the back, respectively. The deposition of *a*-Si:H layers was followed by deposition of 70-nm ITO layers by DC magnetron sputtering (Clusterline tool, Oerlikon) and subsequent deposition of AZO layers by ALD (OpAL reactor, Oxford Instruments). A 300-mm diameter sputtering target with composition of In_2O_3(90 wt %):SnO_2(10 wt%) was used and the sputtering was performed at power of 750 W at temperature of 80 °C. A geometrical conversion (division by 1.7) was used to obtain the thickness of the ITO layer on textured wafer from the thickness of 119 nm measured on flat glass substrate. The ITO and the AZO layers were used in three different cell configurations labeled as "back-AZO cell", "front-AZO cell" and "all-ITO cell" as is depicted in Fig. 1. The back-AZO cells had sputtered ITO on the front side and the front-AZO cells had sputtered ITO at the back side; note that the sputtering of the ITO layers was always done prior to the deposition of the ALD AZO layers. The cells had an area of 10 × 10 cm^2 and were completed by sputtering a full-area silver contact at the back and by screen printing of the collection grid with 3 busbars at the front; the metallization was cured for 10 min at 210 °C. The AZO films were deposited at 200 °C using DEZ, DMAI and H_2O as the precursors, as described in more detail elsewhere [16]. The Al-doping level was controlled by a supercycle approach. The supercycles for different doping levels consisted of single DMAI/H_2O ALD cycles introduced in between 49, 15 or 9 DEZ/H_2O cycles and the cycle ratios 1/50, 1/16 and 1/10 are labeled as "low", "medium" and "high" doping levels, respectively. The average growth per cycle value was 0.16 nm, while the deposition rate was around 0.8 nm/min. The supercycles were repeated to reach a total film thickness of 70–75 nm, as measured on flat Si substrates. The ALD coatings were assumed to have approximately the same thickness on flat and on textured surfaces due to excellent conformality of the ALD technique. Although undoped ZnO was considered too resistive to serve as a front-side TCO, it was applied as a back-side TCO layer.

The influence of the Al-doping level on the optoelectronic material properties of AZO was investigated for as-deposited films grown on Si substrates covered with 450 nm of thermally-grown SiO_2. Room-temperature Hall-effect measurements (Lake Shore 8400 Hall setup), indicated that an increase in Al-doping level lead to an increase in the carrier density values and to a decrease in the mobility values, the latter most likely owing to an increase in ionized-impurity scattering [17] (Table 1). Due to these mutually opposite trends, the film with the medium doping level had the lowest resistivity. Degradation of the electronic properties of the AZO films (bare films without encapsulation) was moderate under regular laboratory ambient conditions, such that over a period of 11 months the sheet resistance values increased by 4.9, 7.6, 0.13 and 2.9% for the undoped, low, medium and high doping, respectively. For the optoelectronic characterization ITO was deposited on *a*-Si(p,i)/glass substrate and annealed at 200 °C. We note that the sheet resistance of ITO on bare glass was four times higher than on *a*-Si (p,i)/glass. While fully understanding this substrate effect would make an interesting future study, the properties measured on *a*-Si(p,i)/glass should give the best representation of our ITO that has been optimized on the basis of cell performance. Hall measurements (Ecopia HMS-3000

Table 1
Electrical properties for the AZO and the ITO thin films as obtained via Hall-effect measurements: sheet resistance (R_{sheet}), resistivity (ρ), mobility (μ) and carrier electron density (n_e). Symbol *d* refers to film thickness.

Al-doping level	*d* (nm)	R_{sheet} (Ω/sq)	ρ (10^{-3} Ωcm)	μ ($cm^2V^{-1}s^{-1}$)	n_e (10^{20} cm^{-3})
undoped	72	880	6.5	28	0.35
low	73	210	1.6	25	1.6
medium	75	110	0.83	14	5.4
high	71	140	1.0	11	5.9
ITO	57	250	1.4	35	1.3

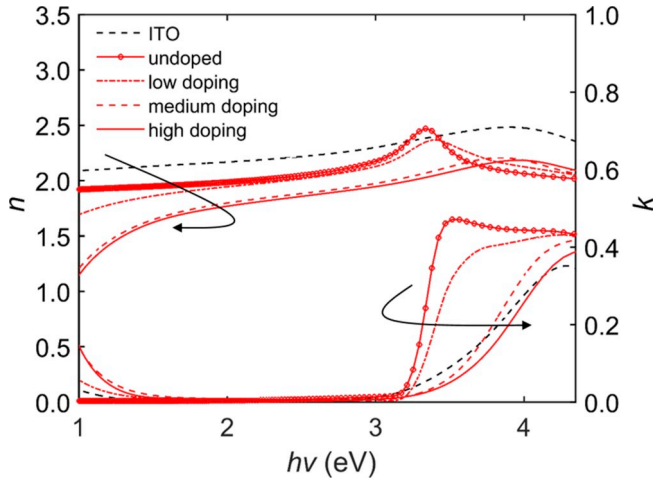

Fig. 2. The refractive index (n) and the extinction coefficient (k) as a function of the energy of the incident light (hv), as determined via spectroscopic ellipsometry for the undoped ZnO film and for the AZO films with low, medium and high Al-doping levels; data is shown also for the ITO film.

Hall setup) indicated that the reference ITO had higher mobility than ZnO and all the AZO layers, as expected, and otherwise properties close to the AZO layer with low doping. As is shown in Fig. 2, the changes in the Al-doping level also led to changes in the optical properties of the films (M − 2000U J. A. Woollam Ellipsometer; CompleteEASE software was used for fitting of the data and a B-spline model was used for the TCO layers). The spectra for the extinction coefficient (k) show that the onsets of the free-carrier absorption (vis-NIR range) and band-gap absorption (UV range) both shifted towards higher energies with increasing Al doping. The latter is due to the rise of the Fermi level deeper into the conduction band, and hence correlates with a decrease in workfunction [18]. Moreover, in the visible range an increase in the doping level led to a decrease in the refractive index (n) owing to higher content of the light Al atoms; further decrease in the spectral region of free-carrier absorption was seen, as n and k are Kramers-Kronig related. For the ITO film vis-NIR absorption was between those of undoped ZnO and AZO with the low doping level; the ITO film had the highest refractive index of all the TCOs studied.

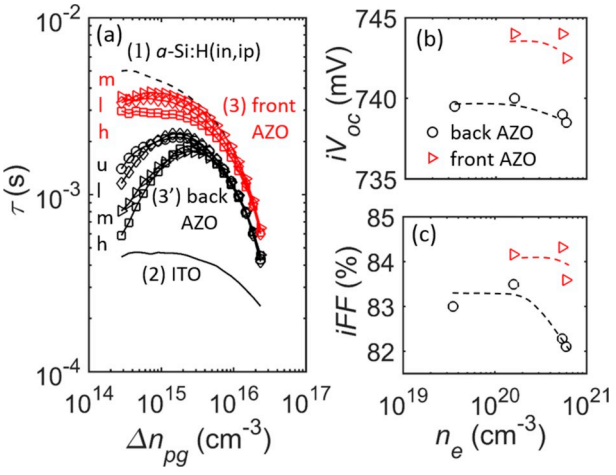

Fig. 3. (a) Lifetime (τ) of photo-generated carriers *vs.* their density (Δn_{pg}); (1) after the deposition of the a-Si:H passivation stacks, (2) after ITO sputtering, and after either (3) the ALD step in the front-AZO configuration or (3′) the ALD step in the back-AZO configuration. **(b)** The implied open-circuit voltage (iV_{oc}) and **(c)** the implied fill factor (iFF) and *vs.* carrier density (n_e) of the AZO layers. The letters u, l, m and h stand for the undoped, low, medium and high doping levels of the AZO layers.

The surface passivation of the cell precursors was studied after different processing steps through photoconductance-decay measurements (WCT-120, Sinton Instruments) that yield the lifetime of the photo-generated charge carriers as a function of their density (Δn_{pg}). After the deposition of the doped a-Si:H layers the lifetime values were above 2 ms at $\Delta n_{pg} \approx 5 \times 10^{15}\,\mathrm{cm}^{-3}$ reflecting high-quality passivation of the c-Si(n) surface (Fig. 3a). Below $5 \times 10^{15}\,\mathrm{cm}^{-3}$ lifetime values increased moderately approaching a value of 5 ms, while above $5 \times 10^{15}\,\mathrm{cm}^{-3}$ lifetime values rapidly decreased owing to Auger recombination. After the deposition of the ITO layers by sputtering, the lifetime values decreased up to one order of magnitude throughout the studied Δn_{pg} range. This can be ascribed to the generation of recombination-active dangling bonds at the a-Si:H(i)/c-Si(n) interface by plasma radiation and ion bombardment [8,19,20]. For a typical cell-fabrication process flow such damage is largely healed, apart from some irreversible microstructural changes, during the curing of the metal contacts at temperatures around 200 °C [3,8].

As the ALD depositions were carried out (subsequently to the ITO sputtering) at temperature of 200 °C, the sputter-induced damage was largely healed during the deposition of the AZO layers. Lifetime values recovered to a large extent owing to the recovery of the chemical passivation [8,19,20]. The lifetime values however depended on the dopant type (n or p) of the a-Si:H layers and the Al-doping level of the AZO layers. For the AZO layers deposited on a-Si:H(n) the recovery in lifetime values was nearly complete and any systematic dependence on the Al-doping level was not observed. High lifetime values at low Δn_{pg} are expected for the AZO/a-Si:H(n) interface as both the materials are n-type and easily form an Ohmic contact [3] (similar behavior is also expected for a-Si:H(n)/ITO contact after exposure to 200 °C [21]). On the contrary, when the AZO layers were deposited on a-Si:H(p) layers, recovery in lifetime values was not complete. Lifetime values were slightly lower overall and particularly below $5 \times 10^{15}\,\mathrm{cm}^{-3}$ lifetime decreased with decreasing Δn_{pg}, such that progressively lower values were seen with increasing Al doping. The decrease in lifetime values at low Δn_{pg} can be ascribed to work-function mismatch between the AZO and the a-Si:H(p) layers [22] and is a sign of degraded field-effect passivation (similar behavior is also expected for a-Si:H(p)/ITO contact after exposure to 200 °C [21]). Such degradation of the field-effect passivation at the AZO/a-Si:H(p) interface can lead to losses in fill factor and even in open-circuit voltage, the latter in the case of a severe workfunction mismatch [12].

The influence of the passivation quality on the fill-factor and open-circuit-voltage losses can be described in terms of implied fill factor and implied open-circuit voltage, quantities that can be extracted from the lifetime data. The latter is primarily sensitive to chemical passivation and the former to the field-effect passivation [21–23]. High implied open-circuit values around 740 mV were seen after deposition of the AZO layers both on p-type or n-type a-Si:H (Fig. 3b). Such high values imply high-quality chemical passivation, while lack of their systematic dependence on the Al-doping level implies absence of severe field-effect passivation losses [12]. The implied voltage values were around 5 mV higher when AZO was deposited on a-Si:H(n) in the front-AZO configuration in comparison to the back AZO configuration with AZO deposited on a-Si:H(p); this difference is discussed in more detail later in the text together with the results for the finalized solar cells. After the deposition of the AZO layers on the a-Si:H(n) layer, the implied fill factor values were 84.0% on average and did not depend systematically on the Al-doping level (Fig. 3c). On the contrary, after the deposition of the ZnO:Al layers on the a-Si:H(p) layer the implied fill factor values decreased from 83.0% to 83.5% for undoped and lowly-doped ZnO to 82.1% for highly-doped ZnO:Al, which implies increased degradation of the field-effect passivation. Such degradation of field-effect passivation underline the need to minimize Al doping at the ZnO:Al/a-Si:H(p) interface—a fact that is enabled by the use of the present rear-emitter configuration.

The finalized solar cells were characterized via current-voltage

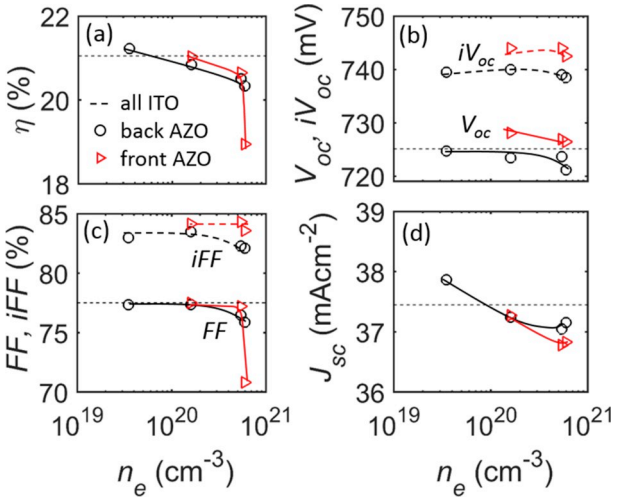

Fig. 4. The one-sun *IV* and the lifetime parameters *vs.* carrier density of the AZO layers (n_e). **(a)** peak conversion efficiency (η), **(b)** open-circuit voltage (V_{oc}) and implied open-circuit voltage (iV_{oc}), **(c)** fill factor (*FF*) and implied fill factor (*iFF*), and **(d)** short-circuit current (J_{sc}). The dashed horizontal lines show the *IV* parameters for the all-ITO reference cell; ITO has carrier density of 1.3×10^{20} cm^{-3}.

measurements under one-sun illumination (WACOM WXS-220S-L2 AM1.5GMM solar simulator). Remarkably, the back-AZO cells and the front-AZO cells both reached efficiency values on par or above that of the benchmark all-ITO cell (Fig. 4a). For both the back-AZO cells and the front-AZO cells the efficiency values increased with decreasing Al doping, such that for the former the highest efficiency of 21.4% was obtained with undoped ZnO, while low Al doping gave the highest efficiency of 21.1% for the latter. These efficiency values are comparable to the values in the range of 21–22% reported for high-efficiency large-area rear-emitter cells with sputtered AZO or ITO as the TCOs and full-area rear metallization [10,24]. The increase in efficiency with decreasing doping level was due to the fact that open-circuit voltage, fill factor and short-circuit current all increased with decreasing Al doping.

The open-circuit voltage values were high in the range of 723–730 mV (Fig. 4b). A small difference between the two configurations was observed, such that for the back-AZO cells the values were systematically 3–5 mV lower than for the front-AZO cells. As a similar difference was seen also for the implied open circuit voltage values, the results imply that the chemical passivation is slightly better in the front-AZO cells. To identify whether this relates to the sputter damage or damage during the ALD deposition, one cell precursor with AZO on both sides of the wafer was characterized by the lifetime measurements. After the deposition of AZO on the front-side *a*-Si:H(n), implied open circuit voltage was measured to be 744 mV, while 747 mV was obtained after subsequent deposition of AZO on *a*-Si:H (p) at the back-side of the cell precursor. This hints that the sputter damage by the ITO deposition leads to more severe recombination at the *a*-Si:H(n)/ITO interface than at the *a*-Si:H(p)/ITO interface. Such could be due to higher defect capture cross section for electrons than for holes [25]. The fact that sputter damage of the *a*-Si(n) was avoided in the front AZO cells led to open circuit voltage values that were higher than those for the ITO reference; this voltage gain compensated for the slight optical losses and was the reason why the cell efficiency of the best front-AZO cell was on par with that of the ITO reference. Overall, the open-circuit values were at a high level owing to the well-preserved chemical passivation.

The fill factor values were generally high in the range of 75–78% (Fig. 4c). As an exception, notably low fill factor was however observed for the front-AZO cells with highly doped AZO. Such could be due to poor lateral charge transport through the TCO, due to e.g. enhanced ionized-impurity and grain-boundary scattering [26]. This can however be excluded as the resistivity for the highly-doped AZO layer is between the resistivity values for the AZO layers with medium and low doping levels, that both yield notably higher fill factor values. Hence, the low fill factor points towards an interface effect such as work-function mismatch or formation of a barrier layer. Based on the implied fill factor values work-function mismatch is not expected for the ZnO:Al/*a*-Si:H(n) interface with highly doped AZO, as (equal to low and medium doping levels) a significant drop in lifetime values is not seen at low Δn_{pg} and implied fill factor is high. This makes formation of a barrier layer the most likely explanation. Indeed, the series resistance (as obtained via the Bowden method [27]) for this cell was 2.61 Ωcm^2, while for all the other front-AZO cells and back-AZO cells the value of series resistance was in the range of 0.92–0.99 Ωcm^2. A plausible explanation for the formation of barrier layer relates to nucleation delay in the ALD growth of ZnO on a-Si:H which we have observed to be more prominent on a-Si:H(n) than on a-Si:H(p). In the case of highly doped AZO only 5 cycles of ZnO are deposited before the first Al_2O_3 doping cycle and it could be that the growth of ZnO is negligible before the first Al_2O_3 cycle. Hence at the a-Si:H/AZO interface AZO could be more Al_2O_3 like than ZnO like and hence form a barrier for charge transport. The fill factor values for the back-AZO cells ranged from 77.7% for undoped ZnO to 76.4% for high Al doping. This trend is in line with the trend for the implied fill factor values, and can hence be explained by decreased field-effect passivation at the AZO/*a*-Si:H(p) contact. Low Al doping thus enables higher fill factor values in particular by mitigating the degradation of field-effect passivation at the AZO/*a*-Si:H(p) contact.

The highest short circuit current values were obtained with undoped ZnO for back-AZO cells and with low Al-doping for the front-AZO cells (Fig. 4d). For the back-AZO cells around 1 mAcm^{-2} and for the front-AZO cells 0.56 mAcm^{-2} was gained by optimizing the doping level. For back-AZO cells it was this optical gain that brought the cell efficiency above that of the ITO reference. The optical gains were confirmed for the front-AZO cells by simulating the optical performance of front-layer stacks based on their refractive indices and extinction coefficients (OPAL2 [28] software). In line with the experimental result, the simulation yielded a current gain of 0.49 mAcm^{-2} when the Al doping level was reduced from medium to low. Based on the simulation the shares of the current gains were 53% for absorption and 47% for reflection. The current gain ascribed to decreased absorption with decreased doping is due to decreased free-carrier absorption [13], also seen as a decrease of the extinction coefficient in Fig. 2. The current gain ascribed to reflection is due to the more optimum refractive index value and hence further improved light incoupling (see also Fig. 2). Moreover, the simulated current gain of 0.49 mAcm^{-2} was not lost when ethyl vinyl acetate (EVA; a common encapsulation material) was used as the incident medium on top of the AZO layers, as in this case a 0.74 mAcm^{-2} gain was obtained. This predicts that the current gains obtained via lower doping of AZO would be maintained in modules as well. As low Al doping is beneficial for maximizing the photocurrent, and at the same low doping does not translate to fill-factor losses, it is evident that the transparence-resistivity tradeoff is minimized in the present rear-emitter cell design.

In conclusion, we demonstrated that ALD-grown AZO can be used in large-area high-efficiency (above 21%) rear-emitter SHJ solar cells as the front-side or the back-side TCO layer. By carefully choosing the solar cell configuration it is possible to mitigate the influence of intrinsically low electron mobility of AZO as well as the work-function mismatch at the AZO/*a*-Si:H(p) interface. Systematic study on the effects of the doping level of AZO indicated that, while low doping is beneficial for optimizing all the cell parameters, the most notable gains are seen for short-circuit current owing to reduced free-carrier absorption and optimized refractive index. Use of low doping for the front-side AZO is enabled by the used rear-emitter configuration in which the conductivity requirement for the front AZO is relaxed. It was shown that the ALD-grown AZO layers can replace sputtered ITO at the front or at the back of the cell without a compromise in the cell efficiency—a fact that indicates the potential for all-AZO (by ALD) ITO-free

cells and hence encourages the use of earth-abundant In-free TCO materials.

Declarations of interest

None.

Acknowledgements

This project has received funding from the European Union's Horizon 2020 research and innovation programme under grant agreement No 641864, INREP project.

Appendix A. Supplementary data

Supplementary data to this article can be found online at https://doi.org/10.1016/j.solmat.2019.109953.

References

[1] K. Yoshikawa, H. Kawasaki, W. Yoshida, T. Irie, K. Konishi, K. Nakano, T. Uto, D. Adachi, M. Kanematsu, H. Uzu, K. Yamamoto, Silicon heterojunction solar cell with interdigitated back contacts for a photoconversion efficiency over 26%, Nat. Energy. 2 (2017) 17032 https://doi.org/10.1038/nenergy.2017.32.

[2] K. Yoshikawa, W. Yoshida, T. Irie, H. Kawasaki, K. Konishi, H. Ishibashi, T. Asatani, D. Adachi, M. Kanematsu, H. Uzu, K. Yamamoto, Exceeding conversion efficiency of 26% by heterojunction interdigitated back contact solar cell with thin film Si technology, Sol. Energy Mater. Sol. Cell. 173 (2017) 37–42 https://doi.org/10.1016/j.solmat.2017.06.024.

[3] S. De Wolf, A. Descoeudres, Z.C. Holman, C. Ballif, High-efficiency silicon heterojunction solar cells: a review, Green 2 (2012) 7, https://doi.org/10.1515/green-2011-0018.

[4] M. Taguchi, A. Yano, S. Tohoda, K. Matsuyama, Y. Nakamura, T. Nishiwaki, K. Fujita, E. Maruyama, 24.7% record efficiency HIT solar cell on thin silicon wafer, IEEE J. Photovolt. 4 (2014) 96–99, https://doi.org/10.1109/JPHOTOV.2013.2282737.

[5] M. Balestrieri, D. Pysch, J.P. Becker, M. Hermle, W. Warta, S.W. Glunz, Characterization and optimization of indium tin oxide films for heterojunction solar cells, Sol. Energy Mater. Sol. Cells 95 (2011) 2390–2399 https://doi.org/10.1016/j.solmat.2011.04.012.

[6] J. Plá, M. Tamasi, R. Rizzoli, M. Losurdo, E. Centurioni, C. Summonte, F. Rubinelli, Optimization of ITO layers for applications in a-Si/c-Si heterojunction solar cells, Thin Solid Films 425 (2003) 185–192 https://doi.org/10.1016/S0040-6090(02)01143-4.

[7] K. Ellmer, Past achievements and future challenges in the development of optically transparent electrodes, Nat. Photonics. 6 (2012) 809 https://doi.org/10.1038/nphoton.2012.282.

[8] B. Demaurex, S. De Wolf, A. Descoeudres, Z. Charles Holman, C. Ballif, Damage at hydrogenated amorphous/crystalline silicon interfaces by indium tin oxide overlayer sputtering, Appl. Phys. Lett. 101 (2012) 171604, https://doi.org/10.1063/1.4764529.

[9] K. Ellmer, Resistivity of polycrystalline zinc oxide films: current status and physical limit, J. Phys. D Appl. Phys. 34 (2001) 3097, https://doi.org/10.1088/0022-3727/34/21/301.

[10] A.B. Morales-Vilches, A. Cruz, S. Pingel, S. Neubert, L. Mazzarella, D. Meza, L. Korte, R. Schlatmann, B. Stannowski, ITO-free silicon heterojunction solar cells with ZnO:Al/SiO_2 front electrodes reaching a conversion efficiency of 23%, IEEE J. Photovoltaics 9 (2019) 34–39, https://doi.org/10.1109/JPHOTOV.2018.2873307.

[11] B. Macco, D. Deligiannis, S. Smit, R.A.C.M.M. van Swaaij, M. Zeman, W.M.M. Kessels, Influence of transparent conductive oxides on passivation of a-Si:H/c-Si heterojunctions as studied by atomic layer deposited Al-doped ZnO, Semicond. Sci. Technol. 29 (2014) 122001 https://doi.org/10.1088/0268-1242/29/12/122001.

[12] M. Bivour, S. Schröer, M. Hermle, Numerical analysis of electrical TCO/a-Si:H(p) contact properties for silicon heterojunction solar cells, Energy Procedia 38 (2013) 658–669 https://doi.org/10.1016/j.egypro.2013.07.330.

[13] Z.C. Holman, M. Filipič, A. Descoeudres, S. De Wolf, F. Smole, M. Topič, C. Ballif, Infrared light management in high-efficiency silicon heterojunction and rear-passivated solar cells, J. Appl. Phys. 113 (2013) 013107, , https://doi.org/10.1063/1.4772975.

[14] M. Bivour, H. Steinkemper, J. Jeurink, S. Schröer, M. Hermle, Rear emitter silicon heterojunction solar cells: fewer restrictions on the optoelectrical properties of front side TCOs, Energy Procedia 55 (2014) 229–234 https://doi.org/10.1016/j.egypro.2014.08.035.

[15] M. Bivour, S. Schröer, M. Hermle, S.W. Glunz, Silicon heterojunction rear emitter solar cells: less restrictions on the optoelectrical properties of front side TCOs, Sol. Energy Mater. Sol. Cell. 122 (2014) 120–129 https://doi.org/10.1016/j.solmat.2013.11.029.

[16] Y. Wu, S.E. Potts, P.M. Hermkens, H.C.M. Knoops, F. Roozeboom, W.M.M. Kessels, Enhanced doping efficiency of Al-doped ZnO by atomic layer deposition using dimethylaluminum isopropoxide as an alternative aluminum precursor, Chem. Mater. 25 (2013) 4619–4622, https://doi.org/10.1021/cm402974j.

[17] K. Ellmer, R. Mientus, Carrier transport in polycrystalline transparent conductive oxides: a comparative study of zinc oxide and indium oxide, Thin Solid Films 516 (2008) 4620–4627 https://doi.org/10.1016/j.tsf.2007.05.084.

[18] E. Burstein, Anomalous optical absorption limit in InSb, Phys. Rev. 93 (1954) 632–633 https://doi.org/10.1103/PhysRev.93.632.

[19] A. Illiberi, P. Kudlacek, A.H.M. Smets, M. Creatore, M.C.M. van de Sanden, Effect of ion bombardment on the a-Si:H based surface passivation of c-Si surfaces, Appl. Phys. Lett. 98 (2011) 242115, https://doi.org/10.1063/1.3601485.

[20] D. Zhang, A. Tavakoliyaraki, Y. Wu, R.A.C.M.M. van Swaaij, M. Zeman, Influence of ITO deposition and post annealing on HIT solar cell structures, Energy Procedia 8 (2011) 207–213 https://doi.org/10.1016/j.egypro.2011.06.125.

[21] A. Tomasi, F. Sahli, J.P. Seif, L. Fanni, S.M. de Nicolas Agut, J. Geissbühler, B. Paviet-Salomon, S. Nicolay, L. Barraud, B. Niesen, S. De Wolf, C. Ballif, Transparent electrodes in silicon heterojunction solar cells: influence on contact passivation, IEEE J. Photovolt. 6 (2016) 17–27, https://doi.org/10.1109/JPHOTOV.2015.2484962.

[22] R. Rößler, C. Leendertz, L. Korte, N. Mingirulli, B. Rech, Impact of the transparent conductive oxide work function on injection-dependent a-Si:H/c-Si band bending and solar cell parameters, J. Appl. Phys. 113 (2013) 144513, https://doi.org/10.1063/1.4799042.

[23] R.A. Sinton, A. Cuevas, Contactless determination of current–voltage characteristics and minority-carrier lifetimes in semiconductors from quasi-steady-state photoconductance data, Appl. Phys. Lett. 69 (1996) 2510–2512, https://doi.org/10.1063/1.117723.

[24] S. Kim, J. Park, P.D. Phong, C. Shin, S.M. Iftiquar, J. Yi, Improving the efficiency of rear emitter silicon solar cell using an optimized n-type silicon oxide front surface field layer, Sci. Rep. 8 (2018) 10657, https://doi.org/10.1038/s41598-018-28823-x.

[25] M. Reusch, M. Bivour, M. Hermle, S.W. Glunz, Fill factor limitation of silicon heterojunction solar cells by junction recombination, Energy Procedia 38 (2013) 297–304 https://doi.org/10.1016/j.egypro.2013.07.281.

[26] V.H. Nguyen, U. Gottlieb, A. Valla, D. Muñoz, D. Bellet, D. Muñoz-Rojas, Electron tunneling through grain boundaries in transparent conductive oxides and implications for electrical conductivity: the case of ZnO:Al thin films, Mater. Horiz. 5 (2018) 715–726, https://doi.org/10.1039/C8MH00402A.

[27] S. Bowden, A. Rohatgi, Rapid and accurate determination of series resistance and fill factor losses in industrial silicon solar cells, Presented at the 17th European Photovoltaic Solar Energy Conference and Exhibition; Munich, Germany; October 22-26, 2001.

[28] K.R. McIntosh, S.C. Baker-Finch, OPAL 2: rapid optical simulation of silicon solar cells, 2012 38th IEEE Photovoltaic Specialists Conference, 2012, pp. 000265–000271, , https://doi.org/10.1109/PVSC.2012.6317616.